Modeling of Electron Cyclotron Resonance Discharges

M. Meyyappan and T. R. Govindan

Abstract—**A simple model to predict the spatially-averaged plasma characteristics of electron cyclotron resonance (ECR) reactors is presented. The model consists of global conservation equations for species concentration, electron density and energy. A gas energy balance is used to predict the neutral temperature self-consistently. The model is demonstrated for an ECR argon discharge. The predicted behavior of the discharge as a function of system variables agrees well with experimental observations.**

I. Introduction

THE current trend in plasma processing is the development of high density plasma sources to achieve high deposition and etch rates, uniformity over large areas, and low wafer damage. Electron cyclotron resonance (ECR) plasma source is one of the candidate technologies [1], [2]. Encouraging results have been reported for ECR deposition of dielectric materials [3], [4] and etching of silicon and III-V compounds [5], [6]. As the technology and applications continue to grow, there is a need to understand the plasma physics and process mechanisms. A growing number of *in situ* diagnostics efforts address this need to enhance the current knowledge of ECR mechanisms. Electron density and temperature measurements have been reported using Thomson scattering [7], microwave interferometry [8], [9] and probes [9]. Ion energy characteristics have been studied in [10]-[12]. Gas heating in ECR plasmas has been observed in [13], [14].

In the past decade, interest in plasma modeling has grown to aid in the interpretation of diagnostics measurements and provide an understanding of the effects of process variables. Various types of models include 1) kinetic simulations which self-consistently predict electron and ion distribution functions, 2) continuum models which solve moment equations, and 3) simplified models which predict spatially averaged properties of interest. Self-consistent, multidimensional computation of both the discharge physics and discharge chemistry for etching and deposition processes using the first two types of models is a complex task and generally not common. In contrast, the third type of model involves simple statements of global conservation of mass and energy of participating species in a prescribed reactor volume and solves a set of algebraic equations (for steady state properties) rapidly [15]. Such zero-dimensional models have long been used in chemical engineering literature for reactor analysis. In plasma processing, [16] used this approach to study plasma etching of Si and SiO_2 and included a very large number of species and reaction set. The model not only provided predictions in reasonable agreement with experiments but also demonstrated a means to study the contribution of various reactions to the overall behavior of the system. The latter is significant since it allows the generation of an "abbreviated reaction set" for use in more sophisticated types of models. Combining with solutions to the Boltzmann equation for the generation of rate coefficients, [17] has effectively used zero-dimensional models to study RF discharges and microwave processing [18]. Recently [19] proposed a global model to study high density discharges. In this paper, we present a zero-dimensional reactor model for ECR processing which includes mass conservation equations for neutral, ionic and electron species, and electron and gas energy balances. We apply the model to both the source and processing chambers to predict the average properties in each of these two regions and compare with available experimental results.

Manuscript received September 9, 1994; revised November 18, 1994. This work was supported in part by the U.S. Army Research Laboratory, Fort Monmouth, NJ.

The authors are with Scientific Research Associates, Inc., Glastonbury, CT 06033 USA.

IEEE Log Number 9412964.

II. Model

We consider spatially averaged properties of the plasma. The balance equations are as outlined in [15]. A mass balance for each of the neutral and ionic species in the plasma is written as

$$\dot{m}(y_{i,\text{in}} - y_i) + VM_i \sum_j R_{ij} + AM_i \sum_K S_{ik} = 0 \quad i = 1, I. \tag{1}$$

Here, the subscript "in" denotes inlet conditions. I is the total number of neutral and ionic species. y_i is the mass fraction of species $i (y_i = \rho_i/\rho)$; ρ_i is the mass density of species i given by $n_i m_i$ where n_i and m_i are the species number density and mass. Other notations are as follows. $\dot{m}$ is the mass flow rate; M_i is the molecular weight; V is reactor volume; A is reactor surface area; R_{ij} is the molar homogeneous reaction rate of species i in reaction j; S_{ik} is the molar heterogeneous reaction rate of species i in surface reaction k. The terms in (1) represent changes due to the flow, species production/consumption due to volume and surface reactions, respectively. In principle, the last term in (1) can be written as two independent contributions from wall and wafer reactions as they may differ in nature. The corresponding surface areas are then $A_{w\ell}$ and A_{wf}, respectively. The net rate of production from volume reactions R_{ij} is written as

$$R_{ij} = (\nu''_{ij} - \nu'_{ij}) \left[k_{fj} \prod_{i+1}^{i=I} (\rho y_i / M_i)^{\nu'_{ij}} - k_{rj} \prod_{i+1}^{i=I} (\rho y_i / M_i)^{\nu''_{ij}} \right].$$

Here, ν_{ij} is stoichiometric coefficient of species i in reaction j. The single and double primes denote reactant and product,

respectively. k_{fj} and k_{rj} are forward and reverse rate coefficients for reaction j. The surface reaction rate is written in a similar manner.

The gas density, ρ is computed from the thermodynamic relation

$$p = RT_g\rho\left[\sum_{i\neq e}\frac{y_i}{M_i} + \frac{T_e}{T_g}\frac{y_e}{M_e}\right] \tag{2}$$

where p is the reactor pressure, R is the universal gas constant, T_g is the gas temperature, T_e is electron temperature and subscript e denotes electrons. The mass flow rate $\dot{m}$ in (1) is taken as constant, though in principle, surface reactions may result in a loss of mass. In such a case, the first term in (1) would be written as $\dot{m}_{\text{in}}y_{i,\text{in}} - \dot{m}y_i$, and $\dot{m}$ then can be obtained from a total mass balance which is the sum of (1) over all I species

$$\dot{m}_{\text{in}} - \dot{m} + A\sum_i M_i\sum_k S_{ik} = 0. \tag{3}$$

The electron number density is obtained from

$$n_e = \sum_{i=1}^{I} q_i n_i \tag{4}$$

where q_i is the charge of species i. Next, we write a plasma power balance

$$P_{\text{ext}} = P_e + P_{\text{ion}} \tag{5}$$

where P_{ext} is the external applied power, and P_e and P_{ion} are power deposited to electrons and ions, respectively. The specifics of the heating mechanism and details of the magnetic field cannot be easily included in a simple, lumped model; external power is merely treated as an input parameter. While it is possible to express P_e in terms of electron conduction current and average electric field, we obtain P_e from an electron energy balance

$$\begin{aligned}&(Qn_e\varepsilon_e)_{\text{in}} - Qn_e\varepsilon_e + P_e - V\tilde{N}\sum_j R_{ej}H_j - 3\left(\frac{m_e}{m}\right)\\ &\times \nu_{e\ell}Vn_ek(T_e - T_g) - A\Gamma_e(\varepsilon_e + 0.5kT_e) = 0.\end{aligned} \tag{6}$$

Here, Q is flow rate given by $\dot{m}/\rho$, ε_e is electron mean thermal energy ($= 3/2kT_e$) where k is Boltzmann constant, $\tilde{N}$ is Avagodro number, R_{ej} is rate of electron impact reaction j, H_j is the corresponding threshold energy, m is mixture-average mass, $\nu_{e\ell}$ is the elastic collision frequency, and Γ_e is electron wall flux. The terms in (6) represent electron energy from inflow and outflow, energy gain from external source, energy loss from all inelastic collisions, energy loss from elastic collisions and energy lost due to electron wall recombination, respectively. The energy of electrons at the wall is $\varepsilon_e + 1/2mv^2$ where v is electron directed velocity; we assume that the electrons at the wall are thermal and rewrite their energy as $\varepsilon_e + 0.5kT_e$. The electron wall flux Γ_e must equal the positive ion wall flux, assuming that the massive negative ions are excluded from the wall due to the positive plasma potential

$$\Gamma_e = \sum\Gamma_+ = (A_{\text{eff}}/A)\sum n_+u_{B+}. \tag{7}$$

Here, the subscript + indicates a positive ion and $\sum$ indicates sum over all positive ions. u_B is the Bohm velocity. Implicit in (7) is the assumption that the ion flux Γ_+ at the wall is the same as that at the edge of the sheath. A_{eff} is an effective area as suggested in [19] to account for the deviation of sheath edge ion density from that at the center

$$A_{\text{eff}} = A_Rh_R + A_Lh_L \tag{8}$$

where A_R and A_L are radial and axial surface areas. The correction factors h_R and h_L are from [20]

$$\begin{aligned}h_R &= 0.8/(4.0 + R/\lambda)^{0.5}\\ h_L &= 0.86/(3.0 + 2L/\lambda)^{0.5}.\end{aligned} \tag{9}$$

h_R and h_L reduce to 0.4 and 0.5 at the free fall limit.

The ion power deposition, P_{ion}, is given by

$$P_{\text{ion}} = A\sum\Gamma_+\Delta\psi \tag{10}$$

where $\Delta\psi$ is the driving potential equal to the difference between the plasma and wall potentials. $\Delta\psi$ can be estimated from (7) by recognizing that

$$\Gamma_e = (n_e/4)v_{e,\text{th}}\exp(-\Delta\psi/kT_e) \tag{11}$$

where $v_{e,\text{th}}$ is electron thermal velocity, $(8kT_e/\pi m_e)^{0.5}$. Combining (7) and (11) we get

$$\Delta\psi = -kT_e\cdot\ln\left[\frac{(A_{\text{eff}}/A)\sum n_+u_{B+}}{(n_e/4)v_{e,\text{th}}}\right]. \tag{12}$$

Combining (5)-(7), (10) and (11), we get the final form of the power balance

$$\begin{aligned}&P_{\text{ext}} + (Qn_e\varepsilon_e)_{\text{in}} - Qn_e\varepsilon_e - V\tilde{N}\sum_j R_{ej}H_j\\ &\quad - 3(m_e/m)\nu_{e\ell}Vn_ek(T_e - T_g)\\ &\quad - A_{\text{eff}}(\varepsilon_e + 0.5kT_e)\sum n_+u_{B+}\\ &\quad + A_{\text{eff}}kT_e\cdot\ln\left[\frac{(A_{\text{eff}}/A)\sum n_+u_{B+}}{(n_e/4)v_{e,\text{th}}}\right]\cdot\sum n_+u_{B+} = 0.\end{aligned} \tag{13}$$

In ECR discharges, it is well known that plasma heating of the gas can result in gas temperatures as high as 1000°K [13], [14]. We write a gas energy balance in order to predict the gas temperature

$$\begin{aligned}&(\dot{m}c_pT_g)_{\text{in}} - \dot{m}c_pT_g + 3(m_e/m)\nu_{e\ell}Vn_ek(T_e - T_g)\\ &\quad + \nu_{ce}Vn_+3/2k(T_+ - T_g) + V\sum_i\bar{h}_iM_i\sum_j R_{ij}\\ &\quad - UA(T_g - T_a) = 0.\end{aligned} \tag{14}$$

Here, c_p is mixture specific heat, $\bar{h}_i$ is species enthalpy per unit mass, ν_{ce} is charge exchange collision frequency, T_+ is ion temperature, U is an overall heat transfer coefficient and T_a is ambient temperature. The terms in (14) represent sensible heat associated with gas inflow and outflow, heat gain due to elastic collisions, heat gain from charge exchange collisions with ions, heat of all other chemical reactions, and finally, heat loss to the ambient, respectively. The last term is written using an overall heat transfer coefficient [21] since the wall temperature is unknown. Representing the heat transfer process by a series

of resistance network, the overall coefficient is given by

$$U = \frac{1}{1/h_i + \Delta x/K + 1/h_0}. \quad (15)$$

Here, h_i and h_0 are convective heat transfer coefficients for gas-wall and wall-ambient conditions, respectively. The middle term in (15) represents conduction through the wall of thickness Δx. K is the thermal conductivity of the wall material. When quartz liners are used in the ECR source chamber as in [14], thermal contact between the liner and the metal chamber wall may not be good; often this results in an additional thermal contact resistance which may be significant. Empirical relations for h_0 can be found in a number of heat transfer texts [21]. We can obtain h_i from kinetic theory for conditions encountered in ECR chambers. The heat transferred by the gas molecules on collision with walls is given by $1/4 n_g v_{\mathrm{th},g} A k (T_g - T_w)$ where n_g is gas number density, $v_{\mathrm{th},g}$ is thermal velocity of gas molecules and T_w is wall temperature. This suggests a relation for h_i as $h_i = 1/4 k n_g v_{\mathrm{th},g}$.

In summary, the reactor model consists of (1)-(4), (13), and (14). We use a code called REAC to solve these equations. REAC is a zero-dimensional reactor analysis code to study plasma and non-plasma reactors. The code has an interpreter that allows input of volume and surface reactions using alphanumeric characters. REAC computes thermochemical properties using NASA Lewis data base. The reverse rate constants are related to equilibrium rate constants ($k_r = k_f/k_{\mathrm{eq}}$) which in turn are computed from a knowledge of standard-state Gibbs free energy. For electron impact reactions, REAC requires rate constants as a function of mean electron energy; if this information is not readily available, a companion zero-dimensional Boltzmann solver may be used to compute the electron energy distribution function (eedf) and rate constants.

III. Results and Discussion

In the present work, we demonstrate the model for an ECR argon discharge. Mass balance for Ar, Ar^+, Ar^*, power balance (13), and gas energy balance (14) are considered. The equations are first solved for the source chamber followed by the solution for the process chamber in a cascading fashion. Volume and surface reactions and the corresponding rate coefficients are from [19]

$e + \mathrm{Ar} \rightarrow \mathrm{Ar}^* + e;$	$3.712 \times 10^{-8} \exp(-15.06/T_e)$
$e + \mathrm{Ar} \rightarrow \mathrm{Ar}^+ + 2e;$	$1.235 \times 10^{-7} \exp(-18.687/T_e)$
$e + \mathrm{Ar}^* \rightarrow \mathrm{Ar}^+ + 2e;$	$2.053 \times 10^{-7} \exp(-4.95/T_e)$
$e + \mathrm{Ar}^* \rightarrow \mathrm{Ar} + e;$	$k = 2 \times 10^{-7}$
$\mathrm{Ar}^* + \mathrm{Ar}^* \rightarrow \mathrm{Ar} + \mathrm{Ar}^+ + e;$	$k = 6.2 \times 10^{-10}$
$\mathrm{Ar}^* + s \rightarrow \mathrm{Ar} + s$	
$\mathrm{Ar}^+ + s \rightarrow \mathrm{Ar} + s.$	

All rate coefficients have units of cm^3/s. s in the above reactions denotes a surface. We assume a unity sticking coefficient for both surface reactions. A constant cross-section of 3.5×10^{-15} cm^2 is assumed for argon-ion charge exchange.

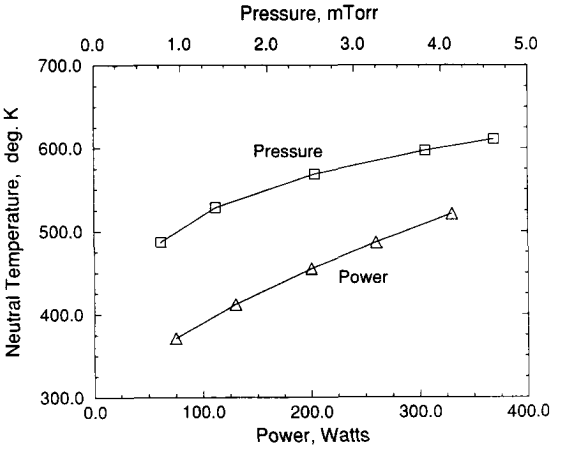

Fig. 1. Gas temperature in the ECR source chamber as a function of pressure and absorbed microwave power. Source diameter = 12.5 cm, length = 15 cm, argon flow = 20 sccm.

Electron elastic collision frequency is given by the relation $\nu_e(\mathrm{Hz}) = 1.756 p/T_g$. The ion temperature is assumed to be 0.5 eV based on the measurements in [14].

Plasma heating of the gas has been known to result in high gas temperatures of about 900°K in ECR source chambers [13], [14]. Hot neutrals and possible high surface temperatures may adversely affect surface reactions. Also, gas heating leads to a reduction in neutral density and affects plasma properties. Hence, we first validate our gas temperature predictions against experimental measurements. Fig. 1 shows predicted gas temperatures as a function of pressure and microwave power for the experimental conditions of [13]. The source chamber is 12.5 cm diameter and 15 cm long. Argon flow is 20 sccm. The uncertainty in the measurements in [13] is dominated by background noise and the error bars span over a 50–80° range [13, (Figs. 4 and 5)]. The predicted temperature in each of the cases in Fig. 1 is well within the error bar and the comparison is good. Ion-neutral charge exchange collision is the major source of gas heating. Electron-gas elastic collisions also lead to a rise in neutral temperature although to a much less extent. The ratio of heat input from charge exchange collisions to that from elastic collisions is about 7–9 for the conditions in Fig. 1. The resultant gas temperature is determined by the effectiveness of heat transfer to the ambient. The gas temperature increases with the absorbed microwave power. This is mainly due to an increase in plasma density with power (as will be seen later). Inspection of (14) reveals that the heating terms are proportional to plasma density. Fig. 1 also shows that the gas temperature increases with chamber pressure. Both collision frequency and plasma density increase with pressure and lead to increased collisional heating. Gas temperatures well above that in Fig. 1 are obtained at higher pressures and power levels; for example, the predicted temperature in the source chamber is 919.5°K at $p = 4.6$ mTorr and absorbed power of 800 W. In contrast, the volume-averaged gas temperature in the process chamber for conditions in Fig. 1 is just above room temperature. Collisional heating in the process chamber is drastically reduced due to a decrease in plasma density. The sensible heat brought into the process chamber by the gas flow is effectively dissipated to the ambient and hence, the gas

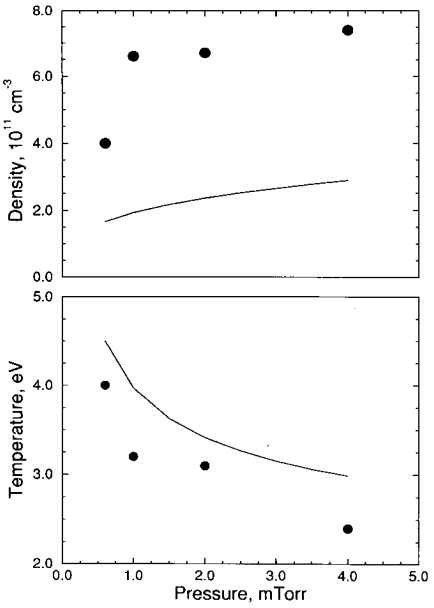

Fig. 2. Pressure dependence of spatially-averaged electron temperature and density (solid line). Also shown (symbols) are Thomson scattering measurements from [7, (Fig. 6)]. The measurements correspond to a small volume on-axis and hence, are quantitatively different from reactor volume-averaged predictions.

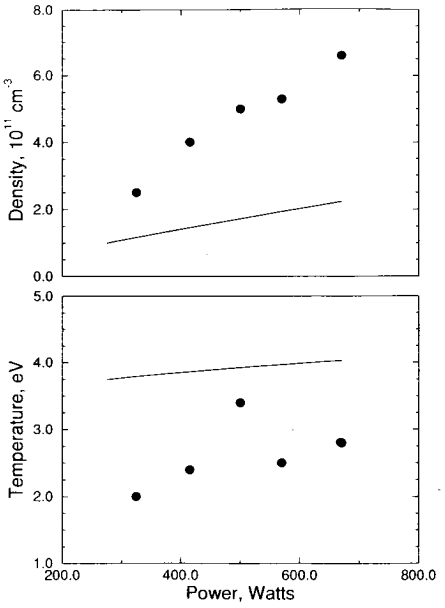

Fig. 3. Variation of spatially-averaged electron density and temperature with absorbed microwave power (solid line). The on-axis experimental measurements from [7, (Fig. 5)] are shown using symbols.

temperature in the process chamber is not much above that of the ambient.

Next we discuss the plasma characteristics predicted by the model. Note that we assume $n_e = n_+$ according to (4). Fig. 2 presents the variation of electron density and temperature with pressure in the source chamber for an absorbed power of 570 W. Fig. 3 presents the plasma characteristics in the source chamber as a function of microwave power at a pressure of 1 mTorr. These results correspond to the experimental conditions of Bowden et al. [7]. The source chamber dimensions are $d = 30$ cm and $\ell = 25$ cm. Argon flow rate is 15 sccm. To understand the discharge behavior, let us inspect (1) for Ar^+ and (13). The Ar^+ density balance requires the generation rate to be equal to the ambipolar loss rate which determines the electron temperature in the discharge. (The flow effects are negligible). Since the particle flux to the wall depends on Bohm velocity as discussed earlier, we note from (1) that $\sqrt{T_e} \cdot \exp(E/kT_e)$ is proportional to $n_g L$ where L is a characteristic length. So, an increase in neutral density would result in a decrease in T_e. The plasma density is determined by (13) which suggests $n_+ = P_{\text{ext}}/f(T_e)$. When the chamber pressure is increased, neutral density increases even with an increase in neutral temperature thus resulting in a drop of electron temperature. The plasma density increases with pressure as shown in Fig. 2. The variation in electron temperature with microwave power is not significant. Any variation seen in Fig. 3 follows changes in gas temperature and thus the neutral density. The plasma density increases with microwave power. Also shown in Figs. 2 and 3 are the electron density and temperature as determined by Thomson scattering measurements from [7]. Note that the measurements correspond to a small plasma volume on the axis of the source chamber and hence, as expected, quantitatively different from the volume-averaged quantities predicted here. But the qualitative behavior is mostly similar with an exception at high microwave powers. The measured density and temperature tend to saturate as power is increased, which has been attributed to the failure of microwaves to propagate in a highly dense plasma [7]. The present model is too simple to account for such phenomena. The present model has also been validated by comparison against Monte-Carlo simulation results of [22]. The quantitative and qualitative agreement between the present model and the volume-averaged results of [22, (Figs. 3 and 7)] are good for the electron temperature dependence on pressure and microwave power. The predictions for the process chamber corresponding to the conditions in Figs. 2 and 3 reveal volume-averaged plasma densities smaller by one to two orders of magnitude and electron temperatures below 2 eV. Note that the product $n_g L$ is higher in the process chamber than that in the source chamber which reduces the electron temperature. The ionization rate in the process chamber also is substantially reduced.

The model also allows an examination of power dissipation in ECR discharges. For a typical case of 1 mTorr and 570 W, the applied power is distributed as follows, from (13):

Electron-gas inelastic collision loss	= 0.4233
Electron-gas elastic collision loss	= 0.0005
Electron amibpolar wall loss	= 0.1562
Electron energy outflow	= 0.0001
Ion acceleration	= 0.4199.

The above distribution essentially does not change when the power is varied from 100 to 700 W at 1 mTorr. However, the distribution is affected by pressure. For example, the fraction of power spent on inelastic collisions goes up from 0.35 at 0.5 mTorr to 0.52 at 5 mTorr while the fraction corresponding to ion acceleration goes down from 0.48 to 0.36. The potential difference $\Delta\psi = V_p - V_f$ from (12) is of the order $5.4kT_e$ with a minor dependence on pressure.

We have used the model to examine the effect of source geometry. Fig. 4 shows the effect of source chamber radius on

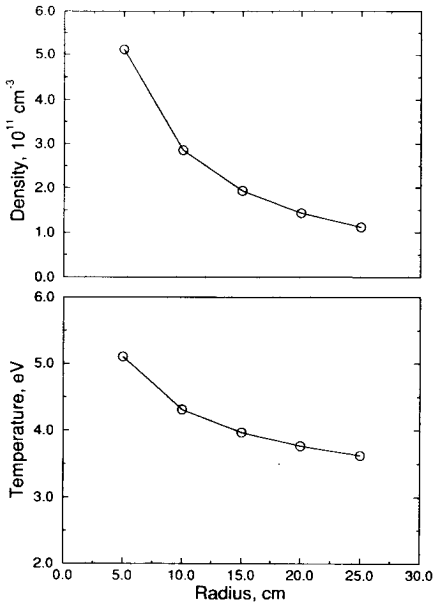

Fig. 4. Effect of source geometry on plasma characteristics. Source chamber length = 25 cm, pressure = 1 mTorr, absorbed power = 570 W and flow rate = 15 sccm.

the plasma characteristics for a source length of 25 cm, at 1 mTorr and 570 W. As the radius is increased, the characteristic length L and product $n_g L$ increase; as discussed earlier, from (1) this requires a decrease in T_e. The volume-averaged plasma density also decreases with an increase in source chamber radius.

IV. Concluding Remarks

We have presented a simple model to predict the volume-averaged properties of an ECR discharge. The model provides spatially-averaged values of electron energy, gas temperature and composition of neutral and ionic species as a function of pressure, absorbed power, flow rates and reactor geometry. In spite of its simplicity, the model would be useful, though to a limited extent, in process and equipment design. The model is built based on global conservation laws and what is already known about the behavior of charged species in the sheaths; in that sense, no new fundamental insights can be derived from such a model. On the other hand, it can provide the global plasma characteristics as a function of system variables in a very efficient manner and be used in a sensitivity study to identify the contribution of various reactions to the overall system behavior. Though the model is demonstrated here only for ECR processing, it applies to other high density discharges as well.

Acknowledgment

The authors acknowledge R. Buggeln for his contributions to the development of REAC and P. Friedland for developing a graphical user interface for REAC. The authors thank C. Lee and M. Lieberman for a copy of their work in [19].

References

[1] J. Asmussen, "Electron cyclotron resonance microwave discharges for etching and thin-film deposition," *J. Vac. Sci. Technol.*, vol. A7, pp. 883–893, 1989.

[2] J. E. Stevens, "Electron cyclotron resonance plasma sources," in *High Density Plasma Sources*, O.A. Popov, Ed. Park Ridge, NJ: Noyes, 1995.

[3] O. A. Popov and H. Waldron, "Electron cyclotron resonance plasma source for plasma enhanced chemical vapor deposition," *J. Vac. Sci. Technol.*, vol. A7, pp. 914–917, 1989.

[4] J. C. Barbour, H. J. Stein, O. A. Popov, M. Yoder, and C. A. Outten, "Silicon nitride formation from a silane-nitrogen electron cyclotron resonance plasma," *J. Vac. Sci. Technol.*, vol. A9, pp. 480–484, 1991.

[5] G. Fortuno-Wiltshire, "Etch characteristics of an electron cyclotron resonance process reactor," *J. Vac. Sci. Technol.*, vol. A9, pp. 2356–2363, 1991.

[6] S. J. Pearton, "Dry-etching techniques and chemistries for III-V semiconductors," *Materials Sci. Eng.*, vol. B10, pp. 187–196, 1991.

[7] M. D. Bowden, T. Okamoto, F. Kimura, H. Muta, K. Uchino *et al.*, "Thomson scattering measurements of electron temperature and density in an electron cyclotron resonance plasma," *J. Appl. Phys.*, vol. 73, pp. 2732–2738, 1993.

[8] S. J. Pearton, T. Nakano, and R. A. Gottscho, "Measurement of electron densities in electron cyclotron resonance plasmas for etching III-V semiconductors," *J. Appl. Phys.*, vol. 69, pp. 4206–4210, 1991.

[9] T. Oomori, M. Tuda, H. Ootera, and K. Ono, "Electrical and optical measurements of electron cyclotron resonance discharges in Cl_2 and Ar," *J. Vac. Sci. Technol.*, vol. 9, pp. 722–726, 1991.

[10] M. Matsuoka and K. Ono, "Magnetic field gradient effects on ion energy for electron resonance microwave plasma stream," *J. Vac. Sci. Technol.*, vol. A6, pp. 25–29, 1988.

[11] W. M. Holber and J. Forster, "Ion energetics in electron cyclotron resonance discharges," *J. Vac. Sci. Technol.*, vol. A8, pp. 3720–3725, 1990.

[12] N. Sadeghi, T. Nakano, D. J. Trevor, and R. A. Gottscho, "Ion transport in an electron cyclotron resonance plasma," *J. Appl. Phys.*, vol. 70, pp. 2552–2569, 1991.

[13] J. Hopwood and J. Asmussen, "Neutral gas temperatures in a mutlipolar electron cyclotron resonance plasma," *Appl. Phys. Lett.*, vol. 58, pp. 2473–2475, 1991.

[14] T. Nakano, N. Sadeghi, and R. A. Gottscho, "Ion and neutral temperatures in electron cyclotron resonance plasma reactors," *Appl. Phys. Lett.*, vol. 58, pp. 458–460, 1991.

[15] M. Meyyappan, "Plasma process modeling," in *Computational Modeling in Semiconductor Processing*, M. Meyyappan, Ed. Norwood, MA: Artech House, 1994.

[16] M. J. Kushner, "A kinetic study of the plasma-etching process. I. A model for the etching of Si and SiO_2 in C_nF_m/H_2 and C_nF_m/O_2 plasmas," *J. Appl. Phys.*, vol. 53, pp. 2923–2938, 1982.

[17] E. S. Aydil and D. J. Economou, "Theoretical and experimental investigation of chlorine RF glow discharges," *J. Electrochem. Soc.*, vol. 139, pp. 1397–1406, 1992.

[18] S. C. Deshmukh and D. J. Economou, "Factors affecting the Cl atom density in a chlorine discharge," *J. Appl. Phys.*, vol. 72, pp. 4597–4607, 1991.

[19] C. Lee, V. Vahedi, and M. A. Lieberman, "Global model of electropositive and electronegative plasmas involving molecular gases," in *45th Gaseous Electron. Conf.*, Montréal, PQ, Canada, Oct. 1993.

[20] V. Godyak, "Non-local bounded plasma model with charge exchange collisions," in *Proceedings X ESCAMPIG*, B. Dubreuil, Ed. Orléans, France: European Physical Society, 1990.

[21] J. P. Holman, *Heat Transfer*. New York: McGraw-Hill, 1976.

[22] Y. Weng and M. J. Kushner, "Electron energy distribution in electron cyclotron resonance discharges for materials processing," *J. Appl. Phys.*, vol. 72, pp. 33–42, 1992.

M. Meyyappan, for a photograph and biography, see this issue, p. 502.

T. R. Govindan received the Ph.D. degree in aerospace engineering from Pennsylvania State University, State College, in 1983.

He is a Senior Research Scientist at Scientific Research Associates, Inc., where he is responsible for developing and applying numerical algorithms for a variety of physical processes. He is currently involved in the development of algorithms for the study of RF discharges, microwave discharges, physics of quantum devices, and fluid mechanics. He has coauthored several publications in these areas.